

# Rotational spectroscopy of AIO

## Low- $N$ transitions of astronomical interest in the $X^2\Sigma^+$ state

O. Launila<sup>1</sup> and D.P.K. Banerjee<sup>2</sup>

<sup>1</sup> KTH AlbaNova University Center, Department of Applied Physics, SE-106 91 Stockholm, SWEDEN, E-mail: olli@kth.se

<sup>2</sup> Astronomy and Astrophysics Division, Physical Research Laboratory, Ahmedabad 380009, Gujarat, INDIA, E-mail: orion@prl.res.in

Received 9 September 2009/ Accepted 9 October 2009

### ABSTRACT

**Aims.** The detection of rotational transitions of the AIO radical at millimeter wavelengths from an astronomical source has recently been reported. In view of this, rotational transitions in the ground  $X^2\Sigma^+$  state of AIO have been reinvestigated.

**Methods.** Comparisons between Fourier transform and microwave data indicate a discrepancy regarding the derived value of  $\gamma_D$  in the  $v = 0$  level of the ground state. This discrepancy is discussed in the light of comparisons between experimental data and synthesized rotational spectra in the  $v = 0, 1$  and  $2$  levels of  $X^2\Sigma^+$ .

**Results.** A list of calculated rotational lines in  $v = 0, 1$  and  $2$  of the ground state up to  $N' = 11$  is presented which should aid astronomers in analysis and interpretation of observed AIO data and also facilitate future searches for this radical.

**Key words.** Molecular data–Molecular processes–Interstellar medium: molecules–Radiolines: stars

## 1. INTRODUCTION

The ground  $X^2\Sigma^+$  state of the AIO radical has been studied with microwave spectroscopy in the  $v = 0, 1$  and  $2$  levels. Törring et al. (1989) recorded the  $N = 1 \rightarrow 2$  transition near 76 GHz. In their Table 1, frequencies for several  $\Delta F = \Delta N$  and  $\Delta F \neq \Delta N$  transitions are shown. Yamada et al. (1990) and Goto et al. (1994) recorded several  $\Delta F = \Delta N$  rotational transitions, resulting in a set of accurate molecular constants, including  $\gamma$  and  $\gamma_D$ .

Launila et al. (1994) have performed a Fourier transform study of the  $A^2\Pi_i \rightarrow X^2\Sigma^+$  transition of AIO in the  $2 \mu\text{m}$  region. In that work, some discrepancies were pointed out regarding their derived  $\gamma_D$  values, as compared to those found in the microwave work. While Yamada et al. (1990) had given a positive value for  $\gamma_D$  for  $v = 0$ , the sign was in fact found to be negative in the light of high- $N$  data of Launila et al. (1994). One of the aims of the present paper is to reinvestigate this discrepancy more closely. The work by Goto et al. (1994), dealing with the  $v = 1, 2$  vibrational levels of the ground state of AIO, does not show the same discrepancy, however.

In a theoretical work, Ito et al. (1994) have discussed and explained the observed vibrational anomalies in the spin-rotation constants of the ground state in the light of spin-orbit interaction with the  $A^2\Pi_i$  and  $C^2\Pi$  states.

Recently, Tenenbaum and Ziurys (2009) reported three rotational transitions of AIO from the supergiant star VY Canis Majoris. In order to facilitate future millimeter-wave search for rotational transitions of AIO, tables containing expected fre-

quencies in the  $v = 0, 1$  and  $2$  levels of the ground state are useful. In the present work, such tables are presented.

## 2. ANALYSIS AND RESULTS

The  $X^2\Sigma^+$  ground state of the AIO radical represents a good example of a Hund's case ( $b\beta_s$ ) coupling. Here, the nuclear and molecular spins  $\mathbf{I}$  and  $\mathbf{S}$  couple to form an intermediate vector  $\mathbf{G}$ , which subsequently couples with  $\mathbf{N}$  to form  $\mathbf{F}$ . Although the energy levels can be calculated with a standard hyperfine Hamiltonian based on  $\mathbf{J} = \mathbf{N} + \mathbf{S}$  formalism, the  $J$  quantum number is to be considered as a bookkeeping device only. This is the case in Table I of Yamada et al. (1990), where both  $J'$  and  $J''$  have been included. Goto et al. (1994) only specify the 'good' quantum numbers  $N$  and  $F$  in their Tables 1 and 2.

In the work of Launila et al. (1994) it was found that the positive sign of  $\gamma_D$  for  $v = 0$  was in conflict with the high- $N$  behavior of the spin doubling of the ground state, as shown in Figs 3 and 4 of their study. We have plotted in the present work the observed  ${}^R Q_{21}$  and  $R_2$  branches in the  $(2,0)$  band of the  $A^2\Pi_i \rightarrow X^2\Sigma^+$  transition from  $N = 3$  to  $N = 104$  (Fig. 1). Here, we are using standard spectroscopic notations, where superscripts in branch designations refer to  $N$ -numbered branch types, while subscripts refer to the spin components. For instance,  ${}^R Q_{21}$  denotes a  $Q$ -branch of  $R$ -type, going from the upper state spin component 2 to the lower state component 1. Vibrational bands are denoted as  $(v_{upper}, v_{lower})$ . From the plot in Fig. 1 we can see that the spin doubling of the ground state  $v = 0$  level increases with  $N$ , up to about  $0.1 \text{ cm}^{-1}$  for  $N = 50$ , after which it starts to decrease until it finally reaches the value of about  $0.07 \text{ cm}^{-1}$  for  $N = 104$ . According to the constants of Yamada et al. (1990), the spin doubling would

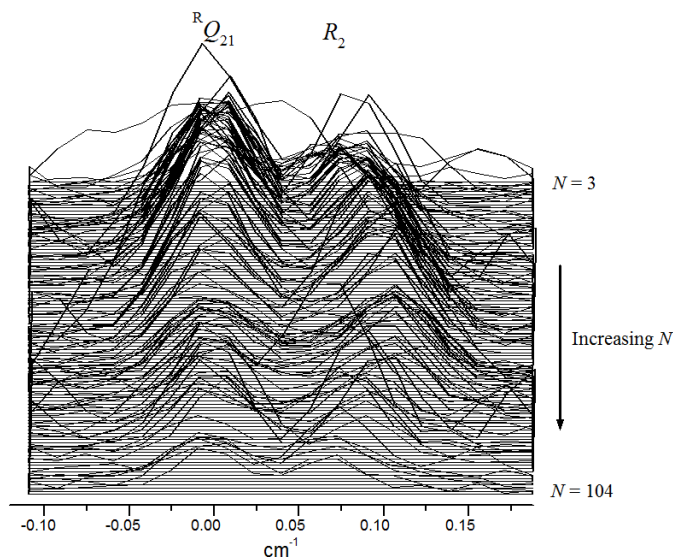


**Fig. 1.** The  ${}^R Q_{21}$  and  $R_2$  branches in the (2,0) band of the  $A^2\Pi_g \rightarrow X^2\Sigma^+$  transition of AIO. The traces show a series of  $0.3 \text{ cm}^{-1}$  intervals, cut directly from the FT spectrum. The  ${}^R Q_{21}$  lines have been arranged so that their reduced wavenumbers coincide. Some lines belonging to other branches are also visible in the plot.

have to increase monotonically to about  $0.3 \text{ cm}^{-1}$ , which is in contrast with the observations.

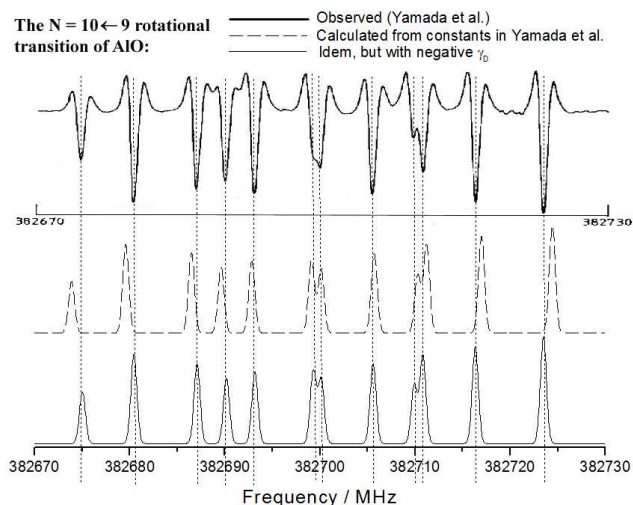


**Fig. 2.** The  $N = 10 \leftarrow 9$  rotational transition in the  $X^2\Sigma^+$  ( $v=0$ ) ground state of AIO from Yamada et al. (1990), as compared with calculated spectra convoluted with a Gaussian line profile of  $0.75 \text{ MHz}$  FWHM.

We have also recalculated the rotational transition  $N = 10 \leftarrow 9$  shown in Fig. 2 of Yamada et al. (1990), using the constants given by them ( $\gamma = 51.660 \text{ MHz}$ ,  $\gamma_D = 0.00343 \text{ MHz}$ ), and also using the same constants, but with a reversed sign of  $\gamma_D$ . The Hamiltonian used was the same as in Launila et al. (1994). The results are presented in Fig. 2.

The uppermost trace of Fig. 2 shows the experimental data, while the middle one shows the recalculated rotational spectrum using the constants of Yamada et al. (1990). The lower trace shows the same spectrum calculated with reversed sign of  $\gamma_D$ . The calculated spectra have been convoluted with a Gaussian profile of  $0.75 \text{ MHz}$  FWHM. It is clear from this comparison that the reversed sign of  $\gamma_D$  results in an almost perfect agreement with the experimental data, while the unaltered constants by Yamada et al. (1990) give rise to deviations of up to  $\pm 1 \text{ MHz}$ . Our conclusion is that the data fit in the work of Yamada et al. (1990) is essentially correct, although the sign of  $\gamma_D$  has to be changed. This sign change alone results in overall deviations of less than  $\pm 0.1 \text{ MHz}$ . However, no new least-squares fit of the data in Yamada et al. (1990) has been performed in the present work. The intensities in the calculated spectra were derived using an intensity formula (B1) from Bacis et al. (1973). Although this formula had actually been written for a Hund's case ( $b\beta_J$ ) - ( $b\beta_J$ ) transition, the agreement with experimental data is surprisingly good.

The calculated frequencies and relative intensities (at  $230 \text{ K}$ ) for all  $\Delta N = \Delta F$  rotational transitions in  $v = 0, 1$  and  $2$  up to  $N' = 11$  are given in Tables 1-3.

### 3. DISCUSSION

The determination of the correct constants for a molecule/radical has its own intrinsic value. Additionally, the present study is also relevant in an astronomical context. Tenenbaum and Ziurys (2009) have recently made the first radio/mm detection of the AIO ( $X^2\Sigma^+$ ) radical toward the envelope of the oxygen rich supergiant star VY Canis Majoris (VY CMa). They observed the  $N = 7 \rightarrow 6$  and  $6 \rightarrow 5$  rotational transitions of AIO at  $268$  and  $230 \text{ GHz}$  and the  $N = 4 \rightarrow 3$  line at  $153 \text{ GHz}$ . While their search for the  $N = 7 \rightarrow 6$  hyperfine transitions was based on direct laboratory measured frequencies by Yamada et al (1990), the search for the  $N = 6 \rightarrow 5$  and  $N = 4 \rightarrow 3$  transitions was based on frequencies calculated from spectroscopic constants of those authors. As has been pointed out, an error is present in one of these constants ( $\gamma_D$  in the  $v = 0$  level of the ground state), which leads to deviations between the calculated and true frequencies. While these deviations are small and may not affect the final result of a line search too seriously, it is still desirable to have accurate frequencies to facilitate future millimeter-wave searches for rotational transitions of AIO. It is planned for several such searches to be taken place in the near future as a consequence of the recent detection in VY CMa. AIO is slowly emerging as a molecule which could attract a fair deal of interest among astronomers. In the VY CMa detection for example it is shown how its study could lead to a better understanding of the gas-phase refractory chemistry in oxygen-rich envelopes. AIO has also been proposed to be a potential molecule in the formation of alumina, which is one of the earliest and most vital dust condensates in oxygen rich circumstellar environments (Banerjee et al. 2007). The mineralogical dust condensation sequence and processes involved are issues of considerable interest to astronomers. The AIO radical also received considerable attention after the strong detection of several  $A \rightarrow X$  bands in the near-infrared ( $1 - 2.5 \text{ microns}$ ) in the eruptive variables V4332 Sgr and V838 Mon (Banerjee et al. 2003; Evans et al 2003). Other IR detections of AIO include IRAS 08182-6000

and IRAS 18530+0817 (Walker et al. 1997). In the optical, the  $B \rightarrow X$  bands have been prominently detected in U Equulei (Barnbaum et al. 1996) and in several cool stars and Mira variables including Mira itself (Keenan et al. 1969; Garrison 1997). J.Chem.Phys. 92(4), 2146

The line lists presented here should also aid in analysis of mm line data for aspects related to kinematics. Since the rotational levels of AIO species are split by both fine and hyperfine interactions, each rotational transition consists of several closely spaced hyperfine components. Figure 2 exemplifies this. If line broadening is small and the spectral resolution of the observations is adequate to resolve these components, then different components will yield different Doppler velocities if the corresponding reference or rest frequencies are in error. This could lead to ambiguity in interpreting the data. Even if the hyperfine components are not distinctly resolved but rather blended to give a composite line profile (as in the observed profiles in VY CMa), modelling of such composite profiles using wrong rest frequencies could lead to errors in estimating the composite line centre, half width of the composite profile and half-widths of the individual hyperfine components. Proper estimates of such kinematic parameters are important as they help determine the size and site of origin of a molecular species. The detailed discussion by Tenenbaum and Ziurys (2009) in the case of VY CMa, which has three distinctly different kinematic flows in the system, illustrates this.

#### 4. SUMMARY

Rotational transitions of AIO have been reinvestigated. The discrepancy regarding the derived value of  $\gamma_D$  of the  $X^2\Sigma^+$  ground state  $v = 0$  level has been shown to be due to a sign error in the microwave work by Yamada et al. (1990). A list of calculated rotational lines in  $v = 0, 1$  and  $2$  of the ground state up to  $N' = 11$  has been presented.

#### 5. REFERENCES

- Bacis, R., Collomb, R. and Bessis, N. 1973, Phys.Rev. A, 8(5), 2255  
 Banerjee, D. P. K., Misselt, K. A., Su, K. Y. L., Ashok, N. M., Smith, P. S. 2007, ApJ, 666, L25  
 Banerjee, D. P. K., Varricatt, W. P., Ashok, N. M. and Launila, O. 2003, ApJ, 598, L31  
 Barnbaum, C., Omont, A. and Morris, M. 1996, A&A, 310, 259  
 Evans, A., Geballe, T. R., Rushton, M. T., Smalley, B., van Loon, J. Th., Eyres, S. P. S., Tyne, V. H. 2003, MNRAS, 343, 1054  
 Garrison, R. F. 1997, JAAVSO, 25, 70  
 Goto, M., Takano, S., Yamamoto, S., Ito, H. and Saito, S. 1994, Chem.Phys.Lett. 227, 287  
 Ito, H. and Goto, M. 1994, Chem.Phys.Lett. 227, 293  
 Keenan, P. C., Deutsch, A. J. and Garrison, R. F. 1969, ApJ, 158, 261  
 Launila, O. and Jonsson, J. 1994, J.Mol.Spectrosc. 168, 1  
 Tenenbaum, E. D. and Ziurys, L. M. 2009, ApJ 694, L59  
 Törring, T. and Herrmann, R. 1989, Mol.Phys. 68(6), 1379  
 Walker, H. J., Tsikoudi, V., Clayton, C. A., Geballe, T., Wooden, D. H., Butner, H. M. 1997, A&A, 323, 442  
 Yamada, C., Cohen, E.A., Fujitake, M. and Hirota, E. 1990,

**Table 1.** Calculated frequencies and intensities of  $\Delta F = \Delta N$  rotational transitions in the  $X^2\Sigma^+$  ( $v=0$ ) ground state of AlO. The constants from Yamada et al. (1990) have been used, with the exception that the sign of  $\gamma_D$  has been reversed. The intensities are calculated according to a Hund's case (b $\beta_J$ ) - (b $\beta_J$ ) formula (B1) from Bacis et al. (1973), at a temperature of 230 K.

G	N'	F'	N''	F''	Freq/MHz	Int. (230 K)
2	1	3	0	2	38 278.080	0.0
3	1	4	0	3	38 281.977	6.0
2	2	2	1	1	76 502.453	0.0
2	2	4	1	3	76 553.373	11.8
3	2	4	1	3	76 559.315	17.7
2	2	3	1	2	76 568.067	4.1
3	2	5	1	4	76 579.518	28.9
3	2	3	1	2	76 677.262	9.4
2	3	5	2	4	114 831.410	43.0
2	3	2	2	1	114 832.298	5.5
2	3	3	2	2	114 835.198	14.1
2	3	4	2	3	114 841.162	26.4
2	3	1	2	0	114 846.559	0.0
3	3	5	2	4	114 850.440	55.2
3	3	6	2	5	114 865.239	76.2
3	3	4	2	3	114 866.448	38.4
3	3	3	2	2	114 888.139	25.1
3	3	2	2	1	114 899.206	15.1
2	4	6	3	5	153 108.310	100.8
3	4	1	3	0	153 109.961	10.3
2	4	5	3	4	153 117.008	73.1
2	4	4	3	3	153 118.588	50.7
2	4	3	3	2	153 121.600	33.2
2	4	2	3	1	153 132.878	19.9
3	4	2	3	1	153 133.226	38.8
3	4	6	3	5	153 133.628	121.9
3	4	5	3	4	153 135.760	94.0
3	4	4	3	3	153 141.151	71.0
3	4	3	3	2	153 142.358	52.6
3	4	7	3	6	153 145.778	155.0
3	5	2	4	1	191 379.947	48.1
2	5	7	4	6	191 382.536	192.2
2	5	6	4	5	191 390.676	151.2
2	5	5	4	4	191 394.726	116.6
3	5	3	4	2	191 398.164	96.1
2	5	4	4	3	191 399.767	88.1
3	5	4	4	3	191 406.813	119.3
3	5	5	4	4	191 409.199	148.4
3	5	6	4	5	191 409.272	183.5
2	5	3	4	2	191 410.177	65.3
3	5	7	4	6	191 411.477	224.7
3	5	8	4	7	191 422.055	272.3
3	6	3	5	2	229 648.771	114.4
2	6	8	5	7	229 653.036	324.2
2	6	7	5	6	229 660.782	267.5
3	6	4	5	3	229 664.971	186.9
2	6	6	5	5	229 665.912	218.4
2	6	5	5	4	229 671.899	176.7
3	6	5	5	4	229 673.641	221.8
3	6	6	5	5	229 677.782	264.1
3	6	7	5	6	229 680.325	313.5
2	6	4	5	3	229 681.974	142.0
3	6	8	5	7	229 684.329	370.3
3	6	9	5	8	229 693.846	434.8
3	7	4	6	3	267 913.912	216.3
2	7	9	6	8	267 918.911	503.3
2	7	8	6	7	267 926.336	428.6
3	7	5	6	4	267 929.255	317.9
2	7	7	6	6	267 931.998	362.9

Table 1. continued.

G	N'	F'	N''	F''	Freq/MHz	Int. (230 K)
3	7	6	6	5	267 938.051	366.9
2	7	6	6	5	267 938.489	305.6
3	7	7	6	6	267 943.172	424.6
3	7	8	6	7	267 947.009	490.7
2	7	5	6	4	267 948.413	256.7
3	7	9	6	8	267 951.860	565.4
3	7	10	6	9	267 960.593	649.0
3	8	5	7	4	306 174.001	360.4
2	8	10	7	9	306 179.316	735.8
2	8	9	7	8	306 186.459	641.1
3	8	6	7	5	306 189.028	495.5
2	8	8	7	7	306 192.386	556.4
3	8	7	7	6	306 197.956	561.0
2	8	7	7	6	306 199.154	481.4
3	8	8	7	7	306 203.668	636.4
3	8	9	7	8	306 208.233	721.4
2	8	6	7	5	306 209.009	416.0
3	8	10	7	9	306 213.497	816.2
3	8	11	7	10	306 221.612	921.0
3	9	6	8	5	344 428.006	553.1
2	9	11	8	10	344 433.426	1028.0
2	9	10	8	9	344 440.311	911.0
3	9	7	8	6	344 443.008	726.3
2	9	9	8	8	344 446.356	805.1
3	9	8	8	7	344 452.051	810.4
2	9	8	8	7	344 453.276	710.3
3	9	9	8	8	344 458.123	905.6
2	9	7	8	6	344 463.087	626.2
3	9	10	8	9	344 463.112	1011.7
3	9	11	8	10	344 468.561	1128.8
3	9	12	8	11	344 476.168	1257.0
3	10	7	9	6	382 675.021	800.6
2	10	12	9	11	382 680.433	1385.7
2	10	11	9	10	382 687.074	1244.3
3	10	8	9	7	382 690.169	1016.2
2	10	10	9	9	382 693.151	1115.3
3	10	9	9	8	382 699.297	1121.2
2	10	9	9	8	382 700.137	998.3
3	10	10	9	9	382 705.589	1238.4
2	10	8	9	7	382 709.915	893.4
3	10	11	9	10	382 710.818	1367.7
3	10	12	9	11	382 716.327	1509.1
3	10	13	9	12	382 723.495	1662.8
3	11	8	10	7	420 914.194	1109.0
2	11	13	10	12	420 919.531	1814.6
2	11	12	10	11	420 925.941	1646.9
3	11	9	10	8	420 929.595	1371.1
2	11	11	10	10	420 931.991	1492.6
3	11	10	10	9	420 938.778	1499.0
2	11	10	10	9	420 938.985	1351.5
3	11	11	10	10	420 945.191	1640.4
2	11	9	10	8	420 948.726	1223.6
3	11	12	10	11	420 950.546	1794.9
3	11	13	10	12	420 956.037	1962.7
3	11	14	10	13	420 962.823	2143.9

**Table 2.** Calculated frequencies and intensities of  $\Delta F = \Delta N$  rotational transitions in the  $X^2\Sigma^+$  ( $v=1$ ) ground state of AlO. The constants from Goto et al. (1994) have been used. The intensities are calculated according to a Hund's case ( $b\beta_j$ ) - ( $b\beta_j$ ) formula (B1) from Bacis et al. (1973), at a temperature of 230 K.

G	N'	F'	N''	F''	Freq/MHz	Int. (230 K)
3	1	4	0	3	37 916.433	6.0
2	1	3	0	2	37 940.955	0.0
2	2	2	1	1	75 811.789	0.0
3	2	4	1	3	75 851.618	17.7
3	2	5	1	4	75 865.649	28.9
2	2	4	1	3	75 868.870	11.8
2	2	3	1	2	75 877.360	4.1
3	2	3	1	2	75 973.826	9.5
2	3	2	2	1	113 785.454	5.5
2	3	3	2	2	113 793.040	14.1
2	3	1	2	0	113 793.103	0.0
3	3	5	2	4	113 794.111	55.3
2	3	5	2	4	113 799.247	43.0
3	3	6	2	5	113 803.169	76.2
2	3	4	2	3	113 803.475	26.4
3	3	4	2	3	113 815.224	38.4
3	3	3	2	2	113 841.408	25.1
3	3	2	2	1	113 857.193	15.1
2	4	3	3	2	151 726.258	33.2
2	4	6	3	5	151 728.377	100.8
2	4	4	3	3	151 728.480	50.8
3	4	6	3	5	151 728.774	121.9
2	4	2	3	1	151 730.961	19.9
2	4	5	3	4	151 731.788	73.1
3	4	1	3	0	151 735.211	10.3
3	4	7	3	6	151 735.526	155.0
3	4	5	3	4	151 735.995	94.1
3	4	4	3	3	151 746.268	71.1
3	4	2	3	1	151 750.044	38.8
3	4	3	3	2	151 752.710	52.6
2	5	7	4	6	189 654.765	192.3
2	5	4	4	3	189 656.532	88.1
2	5	5	4	4	189 656.893	116.7
3	5	2	4	1	189 657.138	48.1
2	5	6	4	5	189 657.809	151.2
3	5	7	4	6	189 658.131	224.8
2	5	3	4	2	189 660.290	65.3
3	5	6	4	5	189 660.900	183.6
3	5	8	4	7	189 663.606	272.4
3	5	5	4	4	189 665.779	148.5
3	5	3	4	2	189 666.704	96.1
3	5	4	4	3	189 668.783	119.3
2	6	8	5	7	227 577.375	324.3
3	6	3	5	2	227 577.836	114.5
2	6	7	5	6	227 580.197	267.6
2	6	6	5	5	227 580.377	218.5
2	6	5	5	4	227 580.899	176.8
3	6	8	5	7	227 582.496	370.5
3	6	7	5	6	227 583.325	313.6
2	6	4	5	3	227 584.223	142.1
3	6	4	5	3	227 585.035	187.0
3	6	6	5	5	227 585.713	264.2
3	6	5	5	4	227 587.022	221.9
3	6	9	5	8	227 587.174	435.0
3	7	4	6	3	265 494.808	216.4
2	7	9	6	8	265 495.305	503.5
2	7	8	6	7	265 497.970	428.9
2	7	7	6	6	265 498.736	363.1
2	7	6	6	5	265 499.743	305.8

Table 2. continued.

G	N'	F'	N''	F''	Freq/MHz	Int. (230 K)
3	7	5	6	4	265 500.733	318.0
3	7	8	6	7	265 501.362	490.9
3	7	9	6	8	265 501.526	565.7
3	7	7	6	6	265 502.401	424.8
3	7	6	6	5	265 502.741	367.1
2	7	5	6	4	265 502.824	256.9
3	7	10	6	9	265 505.661	649.3
3	8	5	7	4	303 406.685	360.6
2	8	10	7	9	303 407.706	736.2
2	8	9	7	8	303 410.250	641.4
2	8	8	7	7	303 411.355	556.7
3	8	6	7	5	303 411.841	495.8
2	8	7	7	6	303 412.650	481.7
3	8	7	7	6	303 413.888	561.4
3	8	9	7	8	303 413.915	721.8
3	8	8	7	7	303 414.147	636.7
3	8	10	7	9	303 414.638	816.7
2	8	6	7	5	303 415.571	416.3
3	8	11	7	10	303 418.377	921.5
3	9	6	8	5	341 312.432	553.4
2	9	11	8	10	341 313.756	1028.6
2	9	10	8	9	341 316.193	911.6
3	9	7	8	6	341 317.083	726.7
2	9	9	8	8	341 317.503	805.7
2	9	8	8	7	341 318.976	710.7
3	9	8	8	7	341 319.162	811.0
3	9	9	8	8	341 319.813	906.2
3	9	10	8	9	341 320.090	1012.4
3	9	11	8	10	341 321.146	1129.5
2	9	7	8	6	341 321.779	626.6
3	9	12	8	11	341 324.576	1257.8
3	10	7	9	6	379 211.141	801.2
2	10	12	9	11	379 212.637	1386.7
2	10	11	9	10	379 214.978	1245.2
3	10	8	9	7	379 215.433	1016.9
2	10	10	9	9	379 216.413	1116.1
3	10	9	9	8	379 217.532	1122.0
2	10	9	9	8	379 217.995	999.0
3	10	10	9	9	379 218.444	1239.3
3	10	11	9	10	379 219.058	1368.7
3	10	12	9	11	379 220.313	1510.2
2	10	8	9	7	379 220.702	894.0
3	10	13	9	12	379 223.494	1664.0
3	11	8	10	7	417 101.951	1109.8
2	11	13	10	12	417 103.541	1816.1
2	11	12	10	11	417 105.791	1648.2
3	11	9	10	8	417 105.972	1372.1
2	11	11	10	10	417 107.299	1493.7
3	11	10	10	9	417 108.077	1500.2
2	11	10	10	9	417 108.943	1352.5
3	11	11	10	10	417 109.166	1641.7
3	11	12	10	11	417 110.003	1796.3
3	11	13	10	12	417 111.379	1964.3
2	11	9	10	8	417 111.564	1224.5
3	11	14	10	13	417 114.346	2145.7

**Table 3.** Calculated frequencies and intensities of  $\Delta F = \Delta N$  rotational transitions in the  $X^2\Sigma^+$  ( $v=2$ ) ground state of AlO. The constants from Goto et al. (1994) have been used. The intensities are calculated according to a Hund's case ( $b\beta_j$ ) - ( $b\beta_j$ ) formula (B1) from Bacis et al. (1973), at a temperature of 230 K.

G	N'	F'	N''	F''	Freq/MHz	Int. (230 K)
3	1	4	0	3	37 542.790	6.0
2	1	3	0	2	37 605.344	0.0
2	2	2	1	1	75 112.495	0.0
3	2	4	1	3	75 137.372	17.7
3	2	5	1	4	75 141.892	28.9
2	2	4	1	3	75 183.222	11.8
2	2	3	1	2	75 183.878	4.1
3	2	3	1	2	75 266.837	9.5
2	3	2	2	1	112 728.294	5.5
2	3	1	2	0	112 728.397	0.0
3	3	6	2	5	112 729.337	76.2
3	3	5	2	4	112 729.778	55.3
2	3	3	2	2	112 742.608	14.1
3	3	4	2	3	112 758.605	38.4
2	3	4	2	3	112 759.967	26.4
2	3	5	2	4	112 763.492	43.0
3	3	3	2	2	112 791.209	25.1
3	3	2	2	1	112 813.425	15.1
3	4	7	3	6	150 311.607	155.1
3	4	6	3	5	150 314.425	122.0
2	4	2	3	1	150 315.892	19.9
2	4	3	3	2	150 318.652	33.2
2	4	4	3	3	150 327.771	50.8
3	4	5	3	4	150 329.449	94.1
2	4	5	3	4	150 338.108	73.1
2	4	6	3	5	150 342.478	100.8
3	4	4	3	3	150 346.552	71.1
3	4	1	3	0	150 358.843	10.3
3	4	3	3	2	150 359.766	52.7
3	4	2	3	1	150 364.690	38.8
3	5	8	4	7	187 889.577	272.5
3	5	7	4	6	187 893.776	224.8
2	5	3	4	2	187 894.977	65.3
2	5	4	4	3	187 898.631	88.2
3	5	6	4	5	187 904.406	183.6
2	5	5	4	4	187 905.924	116.7
2	5	6	4	5	187 913.907	151.3
3	5	5	4	4	187 916.259	148.5
2	5	7	4	6	187 918.686	192.4
3	5	4	4	3	187 926.137	119.4
3	5	2	4	1	187 930.744	48.1
3	5	3	4	2	187 931.560	96.2
3	6	9	5	8	225 462.998	435.2
3	6	8	5	7	225 468.127	370.7
2	6	4	5	3	225 468.664	142.1
2	6	5	5	4	225 472.704	176.9
3	6	7	5	6	225 476.866	313.8
2	6	6	5	5	225 479.119	218.6
2	6	7	5	6	225 486.028	267.7
3	6	6	5	5	225 486.299	264.3
2	6	8	5	7	225 491.071	324.5
3	6	5	5	4	225 494.519	222.0
3	6	4	5	3	225 499.971	187.1
3	6	3	5	2	225 501.378	114.5
3	7	10	6	9	263 031.296	649.6
2	7	5	6	4	263 036.986	257.0
3	7	9	6	8	263 037.118	566.0
2	7	6	6	5	263 041.225	305.9
3	7	8	6	7	263 044.915	491.2

Table 3. continued.

G	N <sup>1</sup>	F <sup>1</sup>	N <sup>2</sup>	F <sup>2</sup>	Freq/MHz	Int. (230 K)
2	7	7	6	6	263 047.148	363.2
3	7	7	6	6	263 053.038	425.0
2	7	8	6	7	263 053.483	429.1
2	7	9	6	8	263 058.730	503.8
3	7	6	6	5	263 060.304	367.3
3	7	5	6	4	263 065.680	318.2
3	7	4	6	3	263 068.245	216.5
3	8	11	7	10	300 593.773	922.1
2	8	6	7	5	300 599.412	416.5
3	8	10	7	9	300 600.162	817.1
2	8	7	7	6	300 603.763	481.9
3	8	9	7	8	300 607.450	722.2
2	8	8	7	7	300 609.381	557.0
3	8	8	7	7	300 614.795	637.1
2	8	9	7	8	300 615.388	641.8
2	8	10	7	9	300 620.807	736.7
3	8	7	7	6	300 621.458	561.7
3	8	6	7	5	300 626.743	496.1
3	8	5	7	4	300 629.976	360.8
3	9	12	8	11	338 149.680	1258.7
2	9	7	8	6	338 155.243	627.0
3	9	11	8	10	338 156.564	1130.3
2	9	8	8	7	338 159.662	711.2
3	9	10	8	9	338 163.572	1013.0
2	9	9	8	8	338 165.085	806.2
3	9	9	8	8	338 170.423	906.8
2	9	10	8	9	338 170.892	912.2
2	9	11	8	10	338 176.469	1029.3
3	9	8	8	7	338 176.685	811.5
3	9	7	8	6	338 181.886	727.2
3	9	6	8	5	338 185.533	553.8
3	10	13	9	12	375 698.240	1665.2
2	10	8	9	7	375 703.724	894.7
3	10	12	9	11	375 705.582	1511.3
2	10	9	9	8	375 708.189	999.8
3	10	11	9	10	375 712.444	1369.6
2	10	10	9	9	375 713.480	1116.9
3	10	10	9	9	375 718.972	1240.2
2	10	11	9	10	375 719.167	1246.1
2	10	12	9	11	375 724.894	1387.7
3	10	9	9	8	375 724.955	1122.8
3	10	8	9	7	375 730.083	1017.6
3	10	7	9	6	375 733.996	801.8
3	11	14	10	13	413 238.667	2147.4
2	11	9	10	8	413 244.076	1225.5
3	11	13	10	12	413 246.449	1965.9
2	11	10	10	9	413 248.572	1353.6
3	11	12	10	11	413 253.247	1797.8
2	11	11	10	10	413 253.773	1494.9
2	11	12	10	11	413 259.391	1649.5
3	11	11	10	10	413 259.559	1643.0
2	11	13	10	12	413 265.266	1817.5
3	11	10	10	9	413 265.343	1501.4
3	11	9	10	8	413 270.411	1373.2
3	11	8	10	7	413 274.505	1110.7